J|A|C|S
ARTICLES
Published on Web 07/08/2006

Application of Centrifugation to the Large-Scale Purification of Electric Arc-Produced Single-Walled Carbon Nanotubes

Aiping Yu,[†] Elena Bekyarova,[†,‡] Mikhail E. Itkis,[†] Danylo Fakhrutdinov,[‡] Robert Webster,[†] and Robert C. Haddon*[,†]

Contribution from the Center for Nanoscale Science and Engineering, Departments of Chemistry and Chemical & Environmental Engineering, University of California, Riverside, California 92521-0403, and Carbon Solutions, Inc., Riverside, California 92506

Received March 24, 2006; E-mail: haddon@ucr.edu

Abstract: We report a further advance in the bulk purification of nitric acid-treated single-walled carbon nanotubes (SWNTs) by use of high-speed centrifugation. We have already shown that low-speed centrifugation is effective in removing amorphous carbon (AC). In these earlier experiments, the AC preferentially suspends in aqueous dispersions on low-speed centrifugation (2000*g*), leaving the SWNTs in the sediment. In a surprising reversal, we now show that high-speed centrifugation (20000*g*) of well-dispersed preparations is effective in sedimenting carbon nanoparticles (CNP), while leaving the SWNTs suspended in aqueous media. Taken together, these two techniques allow the bulk scale (10 g) purification of SWNTs by efficiently separating the two main contaminants, in an industrially viable process. We show that the mechanism of these separations is based on the differential charging (ζ-potential) of the AC, CNPs, and SWNTs that comes about during the chemical processing. Due to their more robust structure, nitric acid oxidation leaves the CNPs with a surface charge density lower than that of the SWNTs, and thus the CNPs do not form stable dispersions in aqueous media during high-speed centrifugation. The efficiency of the process was confirmed by the high purification recovery factor (PRF = 90%), which is a measure of the fractional quantity of the product recovered after the purification. We demonstrate that the purity of SWNTs significantly affects their mechanical and electrical properties.

Introduction

The advancement of the carbon nanotube field in the past decade owes much to the progress made in the purification of single-walled carbon nanotubes (SWNTs). Cutting edge technologies require the use of pure materials, and the continuing efforts to improve the quality of SWNTs emphasize both the difficulty and the importance of this issue.[1−20] Whereas efficient procedures for the purification of SWNTs have been developed in a number of laboratories, technology transfer from the laboratory scale to industrial mass production of purified nanotubes remains problematic and few companies offer rigorously purified SWNTs with appropriate measures of quality assurance. In the absence of such steps, the manufacture of SWNTs will remain a niche industry without widespread application.[21−24] The purification process is complicated by the similarity in the chemical properties exhibited by the nanotubes and the carbonaceous impurities and by the presence of transition metals which are known to be efficient catalysts for the decomposition of carbonaceous materials. This usually results

[†] University of California, Riverside.
[‡] Carbon Solutions, Inc.

(1) Rinzler, A. G.; Liu, J.; Dai, H.; Nikolaev, P.; Huffman, C. B.; Rodriguez-Macias, F. J.; Boul, P. J.; Lu, A. H.; Heymann, D.; Colbert, D. T.; Lee, R. S.; Fischer, J. E.; Rao, A. M.; Eklund, P. C.; Smalley, R. E. *Appl. Phys. A* **1998**, *67*, 29−37.
(2) Bandow, S.; Asaka, S.; Zhao, X.; Ando, Y. *Appl. Phys. A* **1998**, *67*, 23−27.
(3) Dujardin, E.; Ebbesen, T. W.; Krishnan, A.; Treacy, M. M. J. *Adv. Mater.* **1998**, *10*, 611−613.
(4) Dillon, A. C.; Gennett, T.; Jones, K. M.; Alleman, J. L.; Parilla, P. A.; Heben, M. J. *Adv. Mater.* **1999**, *11*, 1354−1358.
(5) Dillon, A. C.; Gennett, T.; Parilla, P. A.; Alleman, J. L.; Jones, K. M.; Heben, M. J. *Mater. Res. Soc. Symp. Proc.* **2001**, *633*, A5.2.1−A5.2.6.
(6) Gorelik, O. P.; Nikolaev, P.; Arepalli, S. *NASA/CR-2000-208926* **2001**.
(7) Chiang, I. W.; Brinson, B. E.; Smalley, R. E.; Margrave, J. L.; Hauge, R. H. *J. Phys. Chem. B* **2001**, *105*, 1157−1161.
(8) Chiang, I. W.; Brinson, B. E.; Huang, A. Y.; Willis, P. A.; Bronikowski, M. J.; Margrave, J. L.; Smalley, R. E.; Hauge, R. H. *J. Phys. Chem. B* **2001**, *105*, 8297−8301.
(9) Banerjee, S.; Wong, S. S. *J. Am. Chem. Soc.* **2002**, *124*, 8940−8948.
(10) Borowiak-Panel, E.; Pichler, T.; Knupfer, M.; Graff, A.; Jost, O.; Pompe, W.; Kalenczuk, R. J.; Fink, J. *Chem. Phys. Lett.* **2002**, *363*, 567−572.
(11) Georgakilas, V.; Voulgaris, D.; Vazquez, E.; Prato, M.; Guldi, D. M.; Kukovecz, A.; Kuzmany, H. *J. Am. Chem. Soc.* **2002**, *124*, 14318−14319.
(12) Harutyunyan, A. R.; Pradhan, B. K.; Chang, J.; Chen, G.; Eklund, P. C. *J. Phys. Chem. B* **2002**, *106*, 8671−8675.
(13) Thien-Nga, L.; Hernadi, K.; Ljubovic, E.; Garaj, S.; Forro, L. *Nano Lett.* **2002**, *2*, 1349−1352.
(14) Sen, R.; Rickard, S. M.; Itkis, M. E.; Haddon, R. C. *Chem. Mater.* **2003**, *15*, 4273−4279.
(15) Zhang, J.; Zou, H.; Qing, Q.; Yang, Y.; Li, Q.; Liu, Z.; Guo, X.; Du, Z. *J. Phys. Chem. B* **2003**, *107*, 3712−3718.
(16) Haddon, R. C.; Sippel, J.; Rinzler, A. G.; Papadimitrakopoulos, F. *MRS Bull.* **2004**, *29*, 252−259.
(17) Xu, Y.; Peng, H.; Hauge, R. H.; Smalley, R. E. *Nano Lett.* **2005**, *5*, 163−168.
(18) Hu, H.; Yu, A.; Kim, E.; Zhao, B.; Itkis, M. E.; Bekyarova, E.; Haddon, R. C. *J. Phys. Chem. B* **2005**, *109*, 11520−11524.
(19) Kim, Y.; Luzzi, D. E. *J. Phys. Chem. B* **2005**, *109*, 16636−16643.
(20) Landi, B. J.; Cress, D. C.; Evan, M. C.; Raffaelle, R. P. *Chem. Mater.* **2005**, *17*, 6819−6834.
(21) Giles, J. *Nature* **2004**, *432*, 791.
(22) Itkis, M. E.; Perea, D.; Jung, R.; Niyogi, S.; Haddon, R. C. *J. Am. Chem. Soc.* **2005**, *127*, 3439−3448.
(23) Arepalli, S.; Nikolaev, P.; Gorelik, O. P.; Nadjiev, V. G.; Holmes, W.; Files, B.; Yowell, L. *Carbon* **2004**, *42*, 1783−1791.
(24) Halford, B. *Chem. Eng. News* **2005**, *84*, 34−35.

10.1021/ja062041m CCC: $33.50

in a low yield of the purified product, the necessity of multistep purification procedures, and difficulties in scaling from the milligram to the gram scale.

As-prepared SWNTs (AP-SWNTs) are typically contaminated with amorphous carbon (AC), catalysts, and graphitic nanoparticles (CNPs).[25−28] Recently we demonstrated an efficient approach for removing the amorphous carbonaceous impurities (AC) from nitric acid treated electric arc-produced AP-SWNTs based on the different ζ-potentials of these two carbonaceous species,[18] by making use of low-speed centrifugation (2000*g*) to remove the AC which preferentially suspends in aqueous media and therefore may be separated from the SWNTs by decantation. We attributed the distinctions in the dispersability characteristics of the SWNTs and AC under low-speed centrifugation to differences in the electrostatic charging as a result of the ionization of surface carboxylic acid groups as measured by the ζ-potentials.

In this study, we focus on the removal of the carbon nanoparticle (CNP) fraction of the impurities in SWNTs. The removal of the CNPs is a particularly challenging task because they are composed of graphitized carbon with few dangling bonds. Their stability is reflected in TGA studies, which show a higher decomposition temperature for the CNPs than the SWNTs, and it is therefore difficult to chemically attack CNPs without damaging or destroying the SWNTs. This has stimulated the search for alternative approaches to the separation of the CNPs from SWNTs, such as filtration in a magnetic field combined with chemical processing.[19]

We report a further advance in the purification of (highly dispersed) nitric acid-treated SWNTs using high-speed centrifugation (20000*g*) to remove the CNPs. We show that, under this force at suitable concentrations, well-dispersed SWNT preparations remain stable, while the CNPs precipitate as sediment allowing their removal by decantation of the supernatant. Taken together, the two processes provide a route for the selective removal of the two main contaminants of nitric acid-treated SWNTs: AC and CNPs. As expected, the resulting purified SWNTs are virtually free from amorphous carbon, catalyst, and graphitic nanoparticles, and in addition the nanotubes are left in a low state of aggregation. We demonstrate that purification improves the mechanical and electrical properties of SWNTs.

Experimental Section

Electric arc-discharge AP-SWNTs were obtained from Carbon Solutions, Inc. (www.carbonsolution.com). The AP-SWNT material was treated with nitric acid and prepurified to remove amorphous carbon as described previously.[18] The prepurified material is denoted as SWNT−COOH. Other chemicals were purchased from Aldrich and used as received.

Sonication was carried out with a bath sonicator, VWR model 550HT with power of 270 W. Near-IR (NIR) spectroscopy was performed on a Varian Cary 500 spectrophotometer. Scanning electron microscopy (SEM) images were taken with a Philips XL-30 microscope. High-resolution transmission electron microscopy (TEM) was performed with a Technai12 instrument operating at 120 kV accelerating voltage. The Raman spectra were recorded on a Bruker FT-IR spectrometer (RFS 100/S) with excitation wavelength of 1064 nm and 200 mW laser power. The thermogravimetric analysis (TGA) was performed at a heating rate of 5 °C/min in air using a Pyris DiamonD thermogravimetric/differential thermal analyzer (TG/DTA) (Perkin-Elmer Instruments). The ζ-potential of aqueous dispersions of individual components (SWNT and CNP) were measured on a zetaplus analyzer (Zetaplus, Brookhaven, NY) at a concentration of 0.05 mg/mL. The stress−strain analysis was carried out in a material testing station (Instron 5543) with extension rate of 0.1 mm/min on samples of dimension 40 mm × 10 mm × 0.05 mm (length × width × thickness). The electrical conductivity was determined by four probe measurement.

The quality of the SWNTs was evaluated from the NIR spectra of dilute dispersions (0.01 mg/mL) of SWNTs in dimethylformamide (DMF), and the relative purity (RP) of all samples was estimated against the reference sample R2 on the basis of the real absorbance in the spectral range of 7750−11 750 cm^{-1}, which covers the S_{22} interband transition of electric arc-produced SWNTs.[16,22,29,30] In general, the starting materials gave values of: AP-SWNTs, RP = 60%; prepurified SWNT−COOH, RP = 110%. RP values higher than 100% correspond to SWNT samples with a relative purity higher than that of the reference sample R2.[29] The efficiency of the purification procedure was evaluated using the purification recovery factor (PRF),[18] which measures the fraction of the desired product that is recovered after the purification with respect to the amount of product initially present in the starting sample. Assuming that a measure of the absolute purity (*P*) is available, then

$$\mathrm{PRF} = [P_{(\mathrm{product})}/P_{(\mathrm{starting\ material})}] \times Y$$

where *Y* is the yield of the product after the purification, defined as weight percentage SWNTs (corrected for the metal content, which is calculated from the residue in the TGA analysis). Clearly an ideal purification process would exhibit *P*(product) ≡ PRF ≡ 100%.

In the case of SWNTs, where the only available quantitative measure of purity is the RP, we write $P = Z \times \mathrm{RP}$, where *Z* is a presently unknown factor with a value smaller than unity. The absolute value of the PRF of every step in a purification procedure can be obtained by the following equation, because it is independent of the Z-factor:

$$\mathrm{PRF} = [P_{(\mathrm{product-SWNT})}/P_{(\mathrm{starting-SWNT})}] \times Y = [\mathrm{RP}_{(\mathrm{product-SWNT})}/\mathrm{RP}_{(\mathrm{starting\ -SWNT})}] \times Y$$

Figure 1 illustrates the purification procedure. In a typical experiment, prepurified SWNT−COOH (10 g, RP = 110%) was bath-sonicated in DI−H_2O (2 L, 3 h) to give a homogeneous dispersion. All experiments were performed at a concentration of 5 mg/mL or less. The SWNT−COOH dispersion was centrifuged at high speed (20000*g*, 60 min). The sediment, collected after decantation of the supernatant, was redispersed in DI−H_2O by sonication (30 min) and centrifuged again. The dispersion−centrifugation−decantation cycle was repeated four times. The supernatant that was decanted and collected on the membrane filter (0.2 μm) contained the purified product: *p*-SWNT−COOH; the sediment remaining after the final centrifugation step mainly consisted of CNPs.

Results and Discussion

The supernatant and sediment fractions collected from the centrifugation of 1 mg/mL dispersions at a centrifugal force of 20000*g* were analyzed using microscopic and spectroscopic techniques to quantitatively and qualitatively evaluate the materials. SEM observations showed that after the centrifugation

(25) Yudasaka, M.; Komatsu, J.; Ichihashi, T.; Achiba, Y.; Iijima, S. *J. Phys. Chem.* **1998**, *102*, 4892−4896.
(26) Yudasaka, M.; Sensui, N.; Takizawa, M.; Bandow, S.; Ichihashi, T.; Iijima, S. *Chem. Phys. Lett.* **1999**, *312*, 155−160.
(27) Bethune, D. S. *Physica B* **2002**, *323*, 90−96.
(28) Itkis, M. E.; Perea, D.; Niyogi, S.; Love, J.; Tang, J.; Yu, A.; Kang, C.; Jung, R.; Haddon, R. C. *J. Phys. Chem. B* **2004**, *108*, 12770−12775.
(29) Itkis, M. E.; Perea, D.; Niyogi, S.; Rickard, S.; Hamon, M.; Hu, H.; Zhao, B.; Haddon, R. C. *Nano Lett.* **2003**, *3*, 309−314.
(30) Zhao, B.; Itkis, M. E.; Niyogi, S.; Hu, H.; Perea, D.; Haddon, R. C. *J. Nanosci. Nanotechnol.* **2004**, *4*, 995−1004.

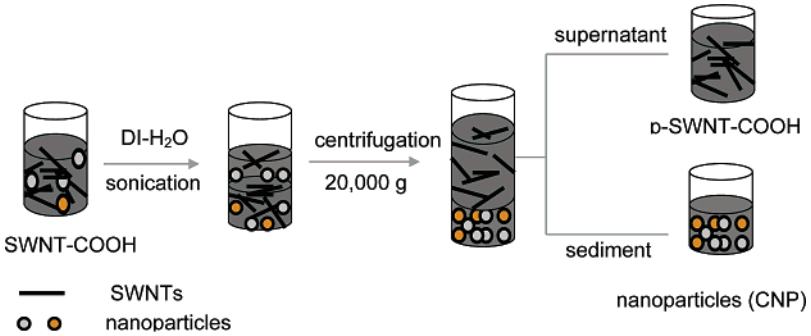

Figure 1. Schematic diagram of the resuspension−centrifugation−decantation cycle for removal of CNPs.

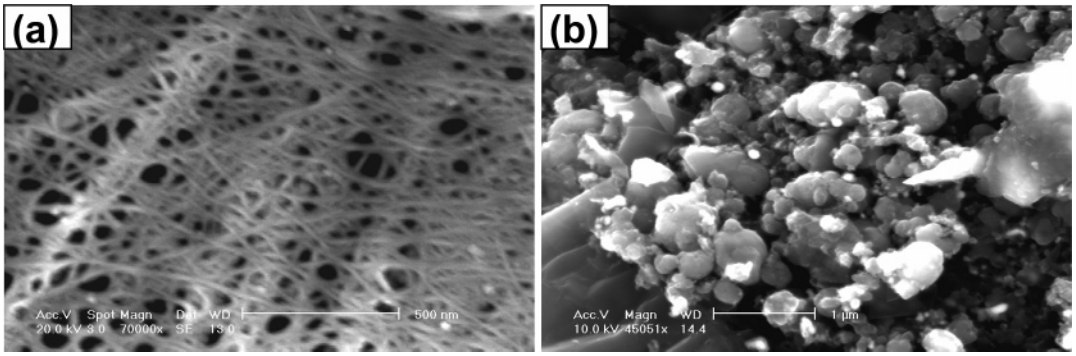

Figure 2. SEM images of materials collected from: (a) the supernatant, showing purified SWNTs and (b) the sediment enriched in nanoparticles (CNPs).

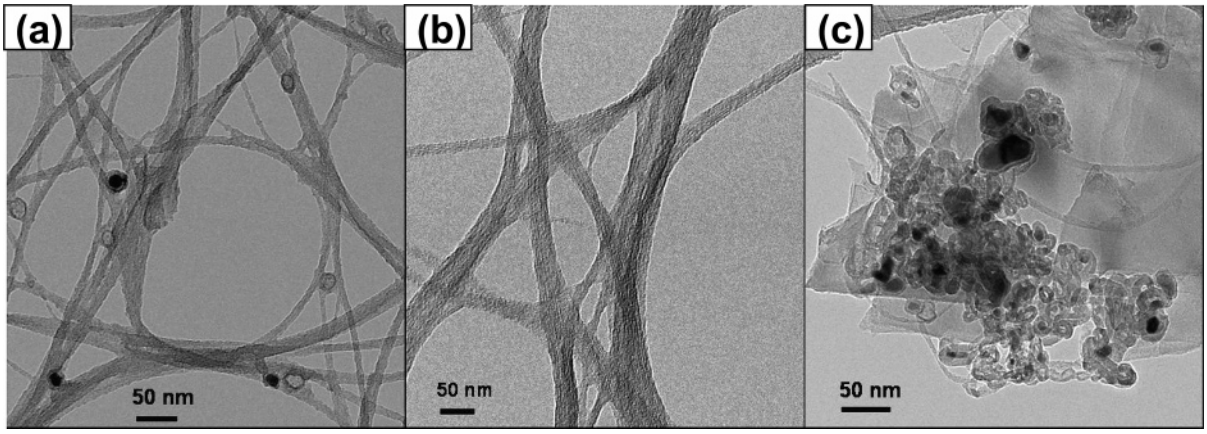

Figure 3. TEM images of: (a) starting SWNT−COOH material showing embedded catalyst nanoparticles, (b) purified *p*-SWNT−COOH fraction, and (c) CNP fraction.

process the supernatant consists mainly of pure SWNTs with very few nanoparticles entrapped between the entangled bundles (Figure 2a), whereas the sediment is enriched in non-nanotube material composed of particles of various sizes (Figure 2b).

Figure 3 shows the TEM micrographs of SWNT−COOH, *p*-SWNT−COOH, and CNP. The presence of nanoparticles attached to the bundles of SWNTs is clearly observed in the starting material, SWNT−COOH (Figure 3a). TEM also reveals that there are two types of nanoparticles: those composed of empty shells and those consisting of metal still encapsulated in graphitic shells.

In the purified material, *p*-SWNT−COOH, nanoparticles were not observed and the nanotubes have smooth, clean surfaces as shown in Figure 3b. The sediment is composed of both graphitic nanoparticles and carbon-coated metal nanoparticles with an average size of 20−50 nm with very few SWNTs visible (Figure 3c).

To analyze the composition of the collected fractions, we used spectroscopic and TGA techniques. The purity of the materials was obtained from the ratio of the area of the S_{22} absorption feature after baseline subtraction (Figure 4a−c, top panels) and the total area under the spectral curve (Figure 4a−c, bottom panels) from solution-phase NIR spectra. The spectral range of 7750−11750 cm^{-1} was used to capture the second interband transition (S_{22}) for semiconducting electric arc-produced SWNTs.[22,29] The starting material used in these experiments (SWNT−COOH) has RP = 110% (Figure 4a), whereas the supernatant was enriched in SWNTs after high-speed centrifugation (20000*g*), giving a final product with RP ≈ 170% (Figure 4b); the sediment showed RP = 5−15%.

The most prominent Raman features related to SWNTs are the tangential mode (G-band) in the vicinity of 1600 cm^{-1} and the low-frequency radial breathing mode (RBM) in the range 100−300 cm^{-1}. The Raman spectroscopy measurements were

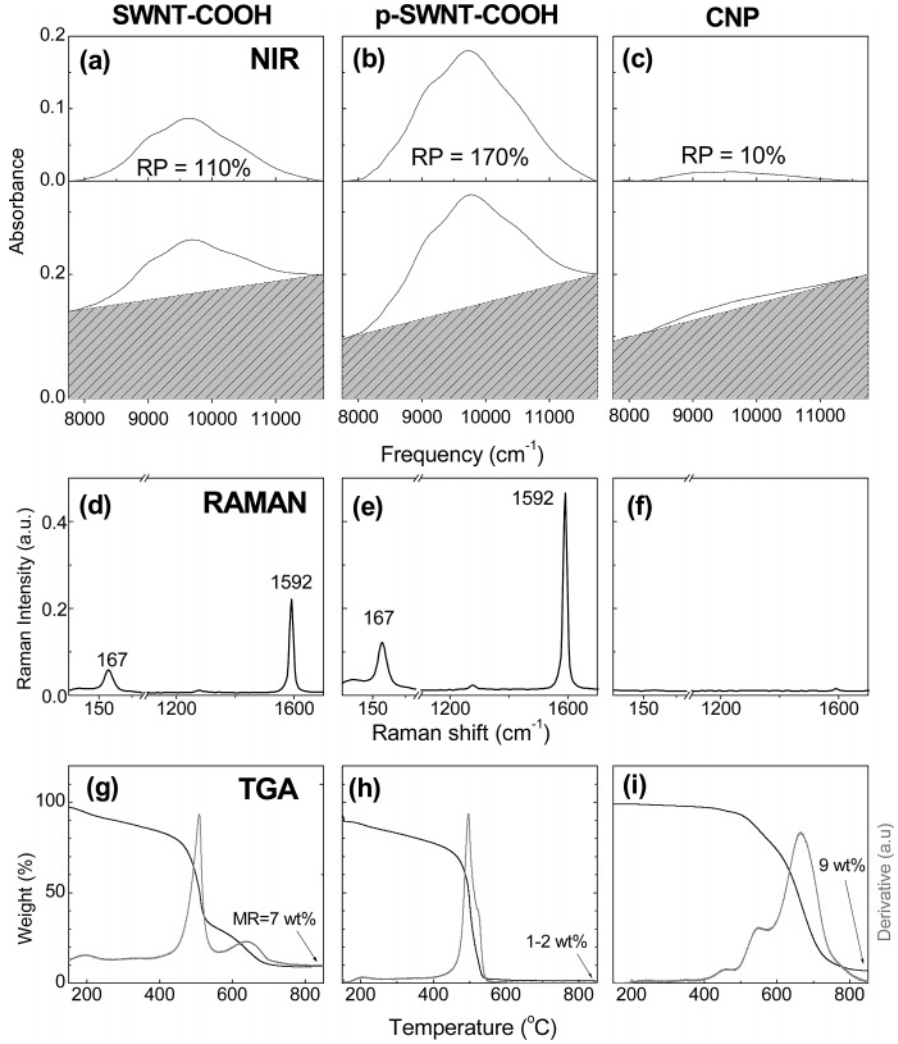

Figure 4. Comparison of the purity of the starting SWNT material (SWNT−COOH), purified SWNT product (p-SWNT−COOH) collected from the supernatant, and the nanoparticle fraction (CNP) collected from the sediment: solution phase NIR spectroscopy (top panel), solution-phase Raman spectroscopy (middle panel), and thermogravimetric analysis (bottom panel). The amount of metal residue (MR) is shown at the high-temperature limit.

conducted using DMF dispersions of the materials with a concentration of 0.005 mg/mL. Due to the resonant nature of the Raman response of SWNTs, the RBM and G-bands are sensitive to the SWNT component in the dispersion and their amplitude is proportional to the SWNT content in each material.[22] The Raman data (Figure 4d−f) confirmed that the highest purity material is associated with the supernatant after the centrifugation (Figure 4e; see starting material in Figure 4d). SWNT Raman features are absent from the sediment (Figure 4f), and it is apparent that this fraction is mainly composed of CNPs.

TGA is a useful tool for providing qualitative information about the purity of SWNTs.[22,23,31] The derivative curve of the starting SWNT−COOH material (Figure 4g) exhibits peaks at 500 and 660 °C due to the combustion of SWNTs and CNPs, respectively. The purified material *p*-SWNT−COOH (Figure 4h) showed only the SWNT-related peak at ∼500 °C, and the absence of a peak around 660 °C confirms the removal of the CNPs, while the sediment fraction was mainly associated with the presence of this component (Figure 4i). The metal content calculated from the residual material in the TGA experiments indicates a decrease from 7% in the starting material (Figure 4g) to 1−2% in the purified product (Figure 4h).

To understand the mechanism of the centrifugal purification of SWNTs, we measured the ζ-potentials of the components; the purification process relies on the relative stabilities of the constituents in the mixture upon application of a gravitational force that is predominantly determined by the net surface charge of a particular component. We have already shown that the different surface charges (ζ-potentials, ζ) at pH 2 allow the efficient separation of the amorphous carbonaceous impurities (AC, $\zeta = -42$ mV) by low-speed centrifugation (2000*g*) and concomitant purification of the SWNTs ($\zeta = -28$ mV).[18] It is important to note that this procedure made use of poorly dispersed SWNTs that were obtained by stirring the nitric acid product, and it is apparent that this is sufficient to disperse the AC but not the SWNTs at low pH values.

The nitric acid treatment leaves the carbon atoms at the nanotube ends and defect sites functionalized with carboxylic acid groups, and it is the ionization of these groups (SWNT−COOH → SWNT−COO^- + H^+) that leads to the presence of a negative charge on the surface of SWNTs.[18] As reflected in the TGA combustion temperatures (Figure 4), the CNPs are more inert than the SWNTs, and thus they are expected to have

(31) Zhang, M.; Yudasaka, M.; Koshio, A.; Iijima, S. *Chem. Phys. Lett.* **2002**, *364*, 420−426.

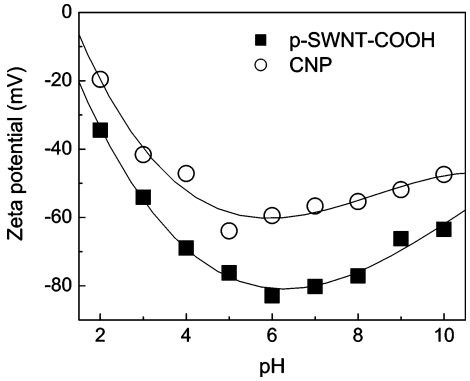

Figure 5. ζ-Potential of *p*-SWNT−COOH and CNP as a function of pH in aqueous dispersion at a concentration of 0.05 mg/mL.

fewer carboxylic acid groups and therefore less net charge than the SWNTs. This is supported by the ζ-potentials given in Figure 5, where it may be seen that for the CNPs, $\zeta = -20$ mV, and for the purified SWNTs (below), $\zeta = -34$ mV, at pH 2. It is interesting to note the shift in ζ-potential of the SWNTs from the value previously reported ($\zeta = -28$ mV)[18] on removal of the CNPs.

To adapt our previous protocol to the problem at hand, it is necessary to find conditions where the SWNTs will remain suspended while allowing the CNPs to accumulate in the sediment, even though both species were previously concentrated in the precipitate under low-speed centrifugation (2000*g*).[18] Surprisingly, we find that highly dispersed preparations give rise to stable suspensions of the SWNTs under conditions of high-speed centrifugation (20000*g*), even though the SWNTs were previously found to be concentrated in the sediment formed when modest force (2000*g*) was applied to unsonicated, stirred preparations.

The most prominent difference in the ζ-potential values of SWNTs and the nanoparticles exists in the pH range between 4 and 8. Typically the aqueous dispersion of SWNT−COOH has pH close to 4, and this naturally falls within the optimum pH range for the separation of SWNTs and CNPs. The high difference in net charge on the surface of SWNTs and nanoparticles, as characterized by the ζ-potential, leads to a distinction in the stability of the two species in aqueous media and facilitates their separation upon application of centrifugal force. It is worth noting that nonfunctionalized SWNTs do not form stable dispersions in water at any concentration and efficient separation of the SWNTs from nanoparticles by centrifugation is not possible.

Process Optimization. To optimize the purification procedure, we studied the effect of the pH, centrifugal force, and dispersion concentration on the separation of SWNTs and nanoparticles.

The net surface charge on the SWNTs depends on the pH of the dispersion;[18] thus by changing the pH of the dispersions it is possible to optimize the separation process during centrifugation. We prepared aqueous dispersions of SWNT−COOH with a concentration of 1 mg/mL and varied the pH in the range between 2 and 10. It is known that within this pH range the nitric acid-treated SWNTs have a high absolute value of ζ-potential and can form stable dispersions in water.[18] The results from experiments conducted at a centrifugation speed of 20000*g* are shown in Figure 6.

The best separation and the highest purity SWNTs are obtained for pH values in the range of 4−7, which coincides with the region of the highest differences in the ζ-potentials (Figure 5) and is also the pH range where the SWNTs have the highest absolute values of the ζ-potential; fortunately, the yield and the RFP of the process reach their optimum values in the same pH range. Because the intrinsic acidity of aqueous dispersions of SWNT−COOH (pH ≈ 4) falls within the optimum pH range for the separation of SWNTs and nanoparticles, the pH of the starting dispersions was not further adjusted in subsequent experiments.

To evaluate the effect of the centrifugal force on the separation of the SWNTs and CNPs, we investigated the influence of this parameter in centrifugation experiments conducted on dispersions with a concentration of 1 mg/mL (Figure 7). Increasing the centrifugation force from 20000*g* to 30000*g* slightly increases the relative purity of the SWNTs, but this improvement occurs at the expense of the yield. On the basis of the PRF, we found that the optimum centrifugal force in this purification process is 20000*g*, which allows a 90% recovery of the SWNTs that are present in the starting sample.

Our initial experiments utilized dispersions with a concentration of 1 mg/mL, and to evaluate the scalability of the process we performed centrifugation experiments using dispersions of higher concentration at the same centrifugation speed (20000*g*). As shown in Figure 8, the increase of the dispersion concentration has a relatively small effect on the relative purity of SWNTs, and on the basis of the data in Figure 8, we conclude that the process remains viable up to starting concentrations of 5 mg/mL. The data clearly demonstrate the industrial viability of the current process: commercial centrifuges are capable of processing 3 L dispersions at 20000*g*, and thus it is possible to purify 10−20 g of SWNTs by application of four cycles of the dispersion−centrifugation−decantation technique reported in the present work.

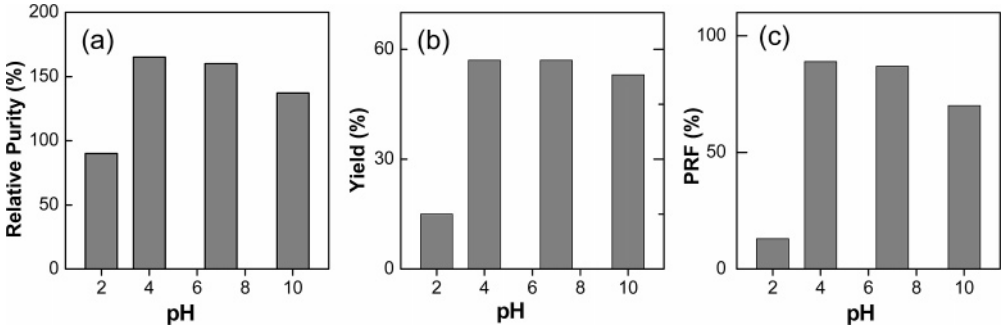

Figure 6. pH dependence of: (a) relative purity, (b) yield, and (c) PRF of the SWNT samples collected from the supernatant after centrifugation.

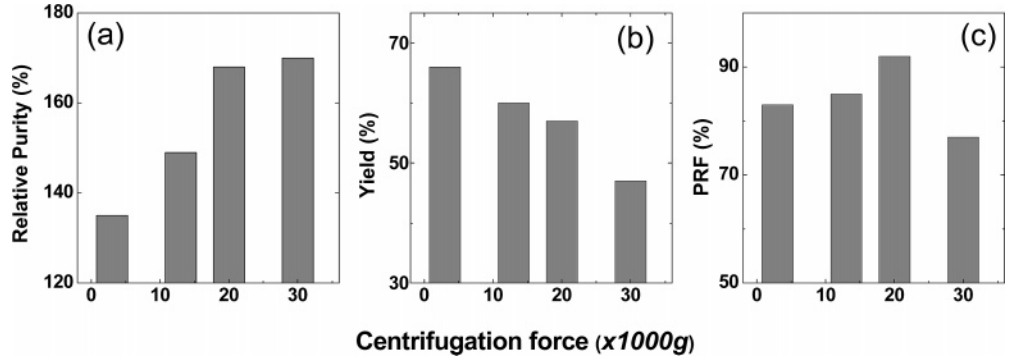

Figure 7. (a) Relative purity, (b) yield, and (c) PRF values of SWNT samples purified at various centrifugation forces.

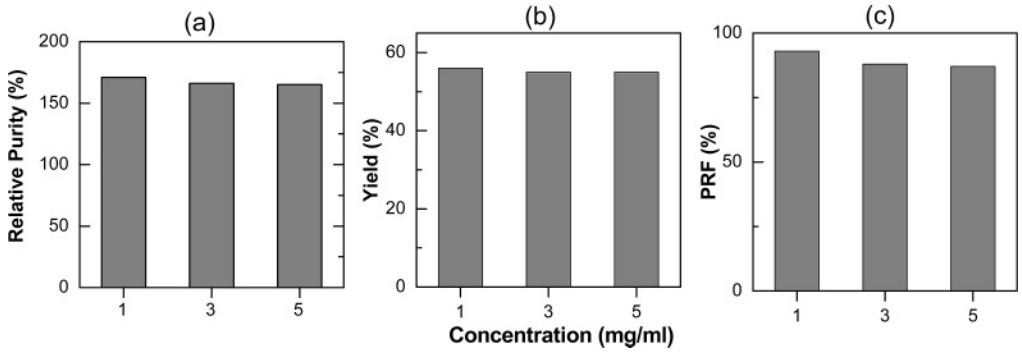

Figure 8. (a) Relative purity, (b) yield, and (c) PRF values of the SWNT samples collected from centrifugation of dispersions with various concentrations.

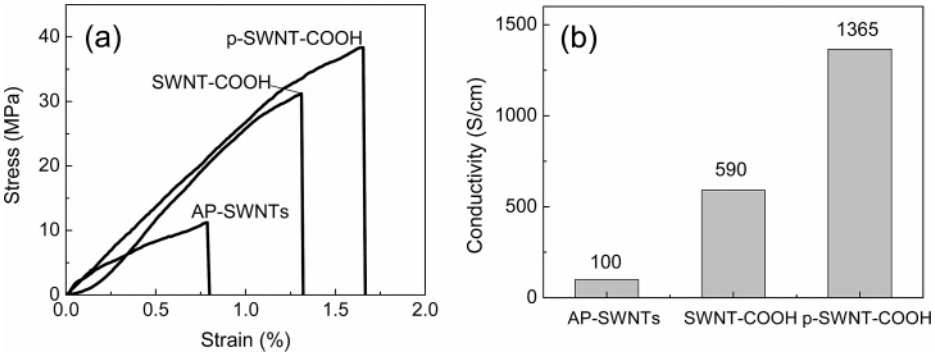

Figure 9. Effect of the purity on the properties of SWNT films: (a) stress−strain curves and (b) room-temperature electrical conductivity of SWNT materials of various purities.

Taking into account the parameters of the first purification step (nitric acid treatment followed by low-speed centrifugation), relative purity, RP = 110%, yield, Y = 25%, and PRF = 65%,[18] we find that the overall performance of the current process (based on AP-SWNT starting material with RP = 60%) gives RP = 160%, Y = 10%, PRF = 50%.

Mechanical and Electrical Properties of Purified SWNTs. It has been suggested that the full realization of the intrinsic properties of SWNTs requires access to high purity materials;[24,32−37] thus it is possible that previous reports on the performance of bulk SWNT samples do not accurately reflect the intrinsic properties of the materials, although we are unaware of previous investigations of this issue. Below we use the mechanical and electrical properties of SWNT materials as a function of purity to demonstrate the important role that purification plays in the performance of SWNTs.

To measure the mechanical and electrical properties, free-standing films of thickness 40−70 μm were prepared by vacuum filtration. The stress−strain curves of AP-SWNTs (RP = 60%), the starting SWNT material used in the purification (SWNT-COOH, RP = 110%), and the material purified by high-speed centrifugation (p-SWNT−COOH, RP = 170%) are illustrated in Figure 9. There is a significant increase in the tensile strength (TS) of the purified SWNT films in comparison to that of the AP-SWNTs; the TS increases from 11.2 MPa for AP-SWNTs to 31.2 and 38.4 MPa for SWNT−COOH and p-SWNT−COOH, respectively. The tensile modulus increases with purity: 1.9 GPa (AP-SWNTs), 2.5 GPa (SWNT−COOH), and 3.1 GPA (p-SWNT−COOH).

(32) Artukovic, E.; Kaempgen, M.; Hetch, D. S.; Roth, S.; Gruner, G. *Nano Lett.* **2005**, *5*, 757−760.
(33) Kaempgen, M.; Duesberg, G. S.; Roth, S. *Appl. Surf. Sci.* **2005**, *252*, 425−429.
(34) Sreekumar, T. V.; Liu, T.; Kumar, S.; Ericson, L.; Hauge, R. H.; Smalley, R. E. *Chem. Mater.* **2003**, *15*, 175−178.
(35) Bekyarova, E.; Itkis, M. E.; Cabrera, N.; Zhao, B.; Yu, A.; Gao, J.; Haddon, R. C. *J. Am. Chem. Soc.* **2005**, *127*, 5990−5995.
(36) Dettlaff-Weglikowska, U.; Skakalova, V.; Graupner, R.; Jhang, S.; Kim, B.; Lee, H.; Ley, L.; Park, Y.; Berber, S.; Tomanek, D.; Roth, S. *J. Am. Chem. Soc.* **2005**, *127*, 5125−5131.
(37) Skakalova, V.; Kaiser, A. B.; Detlaff-Weglikowska, U.; Hrncarikova, K.; Roth, S. *J. Phys. Chem. B* **2005**, *109*, 7174−7181.

The room-temperature electrical conductivities of the films were found to be: AP-SWNTs, $\sigma_{RT} = 100$ S/cm; SWNT−COOH, $\sigma_{RT} = 590$ S/cm; *p*-SWNT−COOH, $\sigma_{RT} = 1365$ S/cm (Figure 9b), and thus the electrical conductivity depends strongly on the relative purity of the SWNT material.

Conclusion

We report the final stage in a two-step process for the bulk purification of SWNTs based on centrifugation that taken together allows the systematic removal of the two most prevalent impurities present in SWNTs, AC and CNPs, on the 10-g scale. Characterization of the product with NIR, TGA, SEM, TEM, and Raman spectroscopy confirms that the SWNTs obtained from this process are almost free of carbonaceous impurities with a residual metal content of ∼1−2 wt %. The purification is based on the different stabilities of dispersions of AC, SWNTs, and CNPs in aqueous media as a result of the different (negative) surface charge. The purity of the SWNTs is shown to play a significant role in their mechanical and electrical performance.

Acknowledgment. This research was supported by DOD/DARPA/DMEA under Award No. DMEA90-02-2-0216. Carbon Solutions, Inc. acknowledges an STTR Phase II Award from the Air Force Office of Scientific Research, No. FA9550-06-C-0004.

JA062041M